

Substrate-Controlled Reorganization of Solution-Grown Polyethylene Single Crystals through Partial Melting

Junichi Nakamura,[†] Masaki Tsuji,[‡] Atsushi Nakayama,[§] and Akiyoshi Kawaguchi^{*,†}

Faculty of Science and Engineering, Ritsumeikan University, 1-1-1 Nojihigashi, Kusatsu, Shiga-ken 525-8577, Japan, Institute for Chemical Research, Kyoto University, Uji, Kyoto-fu 611-0011, Japan, and Department of Chemistry and Chemical Biology, Gunma University, Kiryu, Gunma-ken 376-8515, Japan

Received July 27, 2007; Revised Manuscript Received November 29, 2007

ABSTRACT: By combining transmission electron microscopy (TEM) and atomic force microscopy (AFM), the annealing behavior of polyethylene (PE) single crystals exhibited when annealed on highly oriented pyrolytic graphite (HOPG) was investigated. Morphologically, fibrils were formed and ordered in the form of a leaf venation in an annealed single crystal. From TEM observations, PE chains were found to lay down on the HOPG substrate surface, performing the epitaxial fitting with it; $(110)_{\text{PE}} // (0001)_{\text{HOPG}}$ and $(001)_{\text{PE}} // (11\bar{2}0)_{\text{HOPG}}$. It was also confirmed that in veinlike fibrils forming the venation texture, molecular chains were oriented perpendicular to their length axis. The fibrillar crystals were chain-folded lamellae and were grown edge-on on the HOPG. Molecular orientation was crystallographically adjusted to the substrate *through partial melting* at a temperature below the melting point, performing lattice matching between polymer crystals and the substrate.

Introduction

Polymer crystals are thin lamellae comprising folded chains. The straight stems stand almost perpendicular to the wide flat surface of lamellae. The changes in morphology and physical property by annealing have been studied extensively from the various aspects as described in some monographs.¹ Nowadays, by using an atomic force microscope provided with a high-temperature module, a morphological image can be taken up in a short time and in situ at high temperatures. Consequently, the morphological changes, which polymer crystals exhibit in the process of heating, can be followed in real-time and in situ at high temperatures.^{2–4} In this way, the annealing behavior of polymer crystals can be understood in further detail.

On annealing single crystals of ultralong alkanes on highly oriented pyrolytic graphite (HOPG), fine ribbons or strands were formed and aligned in three definite directions, which differ by $\sim 60^\circ$.² In the case of the annealing of polyethylene (PE) single crystals on a cleavage surface of HOPG, fibrils were formed and arrayed like the venation of a plant leaf.⁴ Thus, it was shown that the HOPG surface induced the specific morphology of PE single crystals on annealing, which was quite different on other various substrates. Morphological changes of solution-grown single crystals of PE and ultralong chain hydrocarbons were followed in real time as a time series of a short period while they were heated.^{5,6} It was found that in the heating process, lamellae start thickening at the periphery and their thickness increased with time and that the fibrillar texture were formed as in the case of annealing of PE single crystals.⁶ Recently, Magonov et al. monitored the morphological changes of PE single crystals in detail using AFM, which occurred when thermally treated on HOPG. They revealed that the transformation in orientation of chain stems in a single crystal, from a normal orientation to a parallel orientation to the substrate, occurred at a temperature as low as 60 °C in a wet state.⁷ Thus,

an atomic force microscope is a very useful tool to investigate the topographic features of polymer crystals. However, with the present resolution of atomic force microscopes, individual molecular chains cannot be determined. To fully understand the annealing behavior of polymer single crystals at a molecular level, it is inevitable to combine TEM with AFM.⁸

Tuinstra and Baer reported that PE was epitaxially crystallized on the graphite surface from the solution.⁹ Also, *n*-alkane crystals were found to grow edge-on on the graphite.¹⁰ Thus, long-chain compounds including PE are arranged in such a way where molecular chains are aligned parallel to the graphite surface. So, to take a molecular image of hydrocarbons, a graphite substrate was used for preparing the samples, where they were deposited and arrayed in a monolayer.^{11,12} The graphite surface was also utilized to orderly arrange other polymers as well as PE, and in some case ribbons were assembled on it.¹³ When PE was crystallized on HOPG from the melt, ribbons were stacked in striation.^{14,15} The morphology was quite similar to the cleavage surface of chain-extended crystals of PE crystallized under high pressure, where bands or ribbons were stacked in layers. It shows three differently oriented ribbons, whose orientations differ by $\pm 60^\circ$. Ultralong chain hydrocarbon also exhibited the stacked-band structure when it was crystallized from the melt.¹⁶ Takenaka et al. investigated the melt-crystallized PE on HOPG and MoS₂ by TEM and reflection high-energy electron diffraction (RHEED), revealing that the PE was crystallized epitaxially in the monoclinic form on HOPG and in the orthorhombic one on MoS₂ only at the interface.¹⁷ In our previous paper, it was shown that the epitaxial crystallization on HOPG occurred at a temperature below the melting point in the process of heating, i.e., through partial melting, as well.⁴ In the present paper, the structure of the venation texture of PE single crystal formed on HOPG by annealing is made clear in combination with AFM and TEM, and its formation mechanism and the effect of the graphite on it are discussed.

Experiments

Polyethylene single crystals were grown by the self-seeding method,¹⁸ using a fractionated PE of $M_n = 32000$ ($M_w/M_n = 1.1$;

* To whom correspondence should be addressed. Fax: +81-(0) 0742-71-8903. E-mail: aki_kawa@kcn.ne.jp.

[†] Faculty of Science and Engineering, Ritsumeikan University.

[‡] Institute for Chemical Research, Kyoto University.

[§] Department of Chemistry and Chemical Biology, Gunma University.

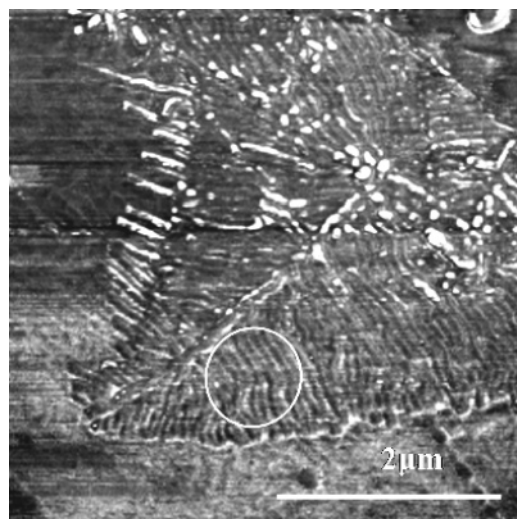


Figure 1. AFM phase image of PE single crystals taken in situ at 126 °C when they were thermally treated on HOPG at the temperature. In the encircled area, fibrils bend in a crankshaft way.

No. 1483 product by NIST). Diamond-shaped and truncated single crystals were grown using the method from both solutions in *p*-xylene and *n*-octane. The endothermic peak on DSC of melting was 128–129 °C. Morphological changes of thus prepared PE single crystals occurring in the process of heating were followed in situ with an atomic force microscope (Digital Instruments, Nanoscope III[®]) equipped with a heating module. Morphology and molecular orientation in annealed PE single crystals were also examined with transmission electron microscopes (JEOL JEM-100C and JEM-200CS). Samples for TEM were prepared as follows. A drop containing suspended PE single crystals was put on a freshly cleaved surface of an HOPG. After the solvent was evaporated, the HOPG with PE single crystals was annealed at a given temperature, e.g., 126 °C, and subsequently, a drop of 10% collodion in isoamyl acetate was put on the HOPG surface at room temperature. After the collodion solution dried up, a dried collodion film was peeled off from the HOPG. In this process, annealed PE single crystals were transferred to the dried collodion film. The surface of the peeled collodion film, which was in contact with the HOPG, was coated with a thin carbon film by evaporation of carbon under a vacuum. A piece of the carbon-coated collodion film was placed on a copper grid for the TEM. Collodion was dissolved away in isoamyl acetate, and then a carbon film with annealed PE single crystals was left on the copper grid.

Results

Figure 1 shows an AFM phase image of PE single crystal, which was taken in situ when heated at 126 °C. A texture like the venation of a plant leaf was formed across the area of the lamellar crystal. Veinlike “fibrillar crystals” in the neighboring sectors, adjoining at the *a*-axis sector-boundary, were arranged in a fairly orderly way and tilted at an angle of ca. 60° to the sector-boundary axis in some parts. The sector boundary axis was a bisector of an angle of ca. 120°, which the fibrils aligned along it in neighboring sectors made. However, fibrils were not always tilted at ca. 60° to the sector-boundary axis in other areas and hence arranged asymmetrically with respect to the sector-boundary. The morphological features of PE single crystals annealed on HOPG are described in more detail in ref 4. Ultralong alkane single crystals also exhibited similar morphological changes when they were thermally treated on HOPG.^{2,6} For alkane crystals, fibrillar or ribbonlike crystals were arranged more regularly. Recently, through detailed AFM observations, Magonov et al. pointed out that fine structural reorganization started at a temperature as low as 60 °C in a wet state when PE

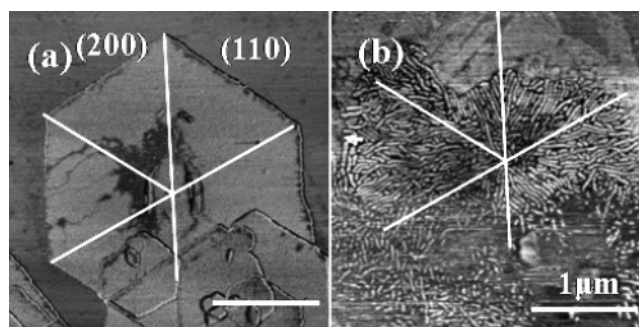


Figure 2. AFM phase images of truncated PE single crystal, taken (a) at room temperature and (b) in situ at 126 °C. Both images were taken from the identical area. The notations (200) and (110) in part a denote the sectors. Lines show the sector boundaries.

single crystals were annealed on the HOPG and that the venation texture was made as a result of major transformation. Fine fibrils, called “strands” or “ribbons” by Magonov et al., extended from the periphery at around 90 °C even in a dried state.⁷

From the periphery of the single crystal in Figure 1, fine fibrils extend in the direction different from that of the length axis of interior veinlike fibrils. The fine fibrils were ~10 nm wide and 10 nm thick. The fibrils extended further with isothermal heating and became wider and thickened when the annealing temperature increased. From the morphological features, we see that PE chains flowed out of the lamellar crystal due to the fibrillar extension. As a result, the lamellar thickness decreased on annealing on the HOPG. Ultralong chain hydrocarbon behaved similarly when annealed.^{6,7} Ordinarily, lamellar polymer crystals increased their thickness from their periphery and with time through heat treatment.^{1,5}

Figure 2 compares an AFM phase image of an as-grown truncated PE single crystal (Figure 2a) and one after it was annealed at 126 °C (Figure 2b). Though largely deformed, annealed crystals comprise fine fibrils. The fibrils are arranged in a fairly orderly way. It is to be noted here that fibrils in the respective sectors of the annealed crystals are arranged with their length axis roughly normal to the lateral surface of the original truncated crystals. It means that fine ribbons formed in the {200} sector are aligned with their length axis parallel to the *a*-axis sector boundary. The morphological features are seen more definitely in Figure 5 of ref 5: Thus, it is likely that fibrils are formed to orient their length axis in the direction perpendicular to the lateral surface of the original crystal.

To clearly understand the molecular orientation in the fibrils, annealed PE single crystals were examined through a TEM. Parts a and b of Figure 3 show, respectively, an electron micrograph and the corresponding electron diffraction pattern of a PE single crystal, which was annealed on HOPG at 126 °C. The electron diffraction pattern is the same as those of PE crystals grown on HOPG from the solution⁹ and the melt.¹⁷ Seemingly, the pattern is complicated as seen in Figure 3b. As discussed later, however, a set of slightly arced reflections originating from the PE crystal, are put on a specific reciprocal lattice net and indexed on the basis of the orthorhombic unit cell¹⁹ as shown in Figure 3c. The indexing explains that PE chains lay down parallel to the HOPG surface, aligning parallel to the crystallographic [11 $\bar{2}$ 0] direction of hexagonal HOPG lattice.

Figure 4 shows an electron micrograph of a single crystal, which was annealed on a HOPG at 126 °C for 10 min, and the corresponding selected-area electron diffraction pattern. A fine venation texture was formed in such a way where constituent fibrils were fairly ordered with their length axis perpendicular

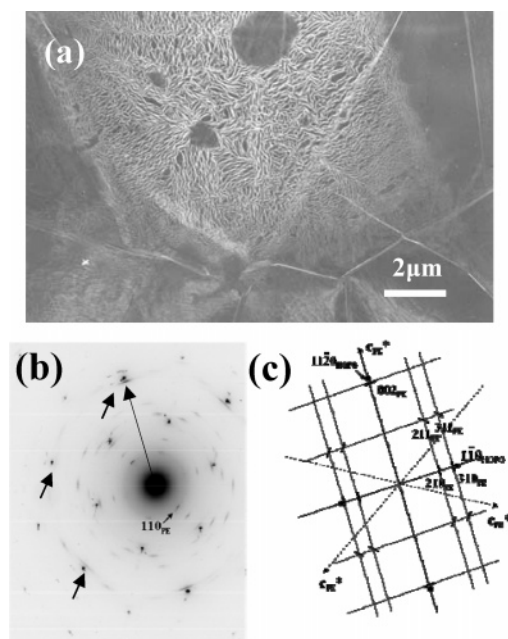


Figure 3. (a) TEM image of a PE single crystal annealed on a HOPG at 126 °C. (b) Electron diffraction pattern corresponding to the image. Arrowed spots indicate the 002 reflections of PE. (c) Reciprocal lattice net corresponding to the orientation of the arrowed c^* -axis in part b. Two other c^* -axes in (b) are shown with dotted lines, rotated by $\pm 120^\circ$.

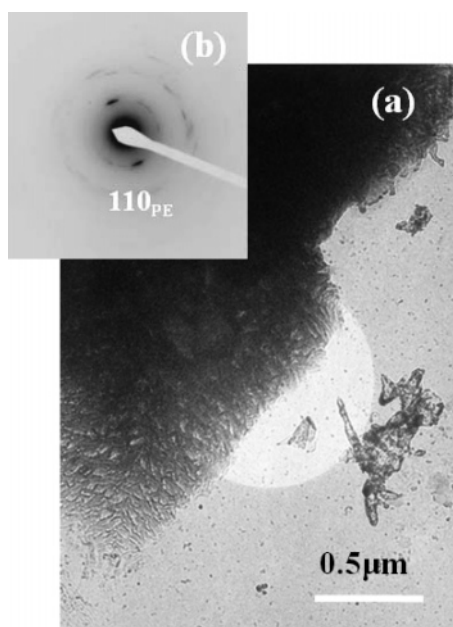


Figure 4. Selected-area electron diffraction pattern (b) corresponding to the encircled area in a TEM photograph (a) of a PE single crystal, which was annealed at 126 °C for 10 min.

to the edge of the lamellar crystal. The 110_{PE} reflection was strongly observed. In Figure 3b, however, the reflection was not observed or very weak. It is considered that when an annealed PE lamella was adhered to the HOPG substrate, the 110_{PE} reflection was not or weakly observed because the {110}_{PE} plane was tilted a little from the normal to the HOPG substrate. Lamellae were disordered when it was taken off from the substrate in the process of preparing the sample, and consequently constituent fibrils had the orientation of giving the 110_{PE} reflection accidentally. Even so, this did not affect the relationship in orientation of the molecular chains within the PE fibrils. As the 101_{PE} reflection was observed, it is still

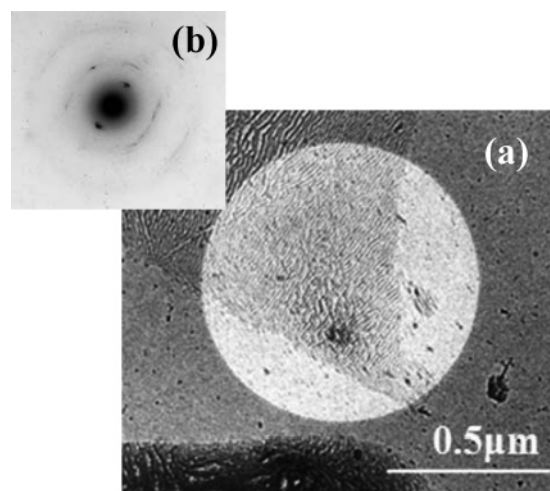


Figure 5. Selected-area electron diffraction pattern (b) corresponding to the encircled area in a TEM photograph (a) of a PE single crystal, which was annealed at 126 °C. The electron diffraction pattern is like a fiber pattern. The fiber axis is almost perpendicular to the length axis of fibrils, which run from the upper-right to the lower-left in part a.

warranted that PE chains aligned parallel to the substrate surface. Figure 5 shows another set of an electron micrograph and the corresponding selected-area electron diffraction pattern. In Figure 5, fibrils are oriented perpendicular to the right lateral surface of the original diamond-shaped crystal lamella, not to the right side, and run in the same direction over the selected area across the sector-boundary. Even though, the selected-area electron diffraction pattern is similar to a fiber pattern, in which the c^* -axis is perpendicular to the fibrillar length. Thus, it is concluded that PE chains should be oriented perpendicular to the length axis of fibrils, lying down on the HOPG substrate.

Discussion

Intense sharp spots in Figure 3b are originated from the HOPG substrate. From their indexing, it is confirmed that the substrate surface is the (0001) plane. The slightly arced reflections in Figure 3b arose from PE crystals and were indexed on the basis of the orthorhombic unit cell.¹⁷ The 002_{PE} reflection is seen in the direction parallel to the 112_{HOPG} reflection, and the 210_{PE} and 310_{PE} reflections are identified in the direction perpendicular to that of the 002_{PE} reflection or in the direction of 1100 HOPG spot.^{9,15} (Here, the suffix denotes the kind of crystal causing the corresponding reflection.) Such a reciprocal lattice net as sketched in Figure 3c is constructed for the above indexing of PE reflections, and some of PE reflections in Figure 3a can be explained. The 002_{PE} reflection is observed in the two other directions as indicated by arrows in Figure 3b. The c^* -axes for the reflections are denoted by dotted lines in Figure 3c, which are rotated by $\pm 120^\circ$ from the c^* -axis of the reciprocal net of Figure 3c. Thus, the whole electron diffraction pattern in Figure 3b is reproduced by superimposing two reciprocal nets similar to Figure 3c, on the net of Figure 3c as follows: their c^* axes coincide with the dotted c^* -axes in Figure 3c.

The 210_{PE} and 310_{PE} reflections were very frequently observed in the three directions. On the contrary, the 110_{PE} reflection was sometimes identified as indicated with a thin arrow in Figure 3b. This implies that as the (110)_{PE} plane or (110)_{PE} plane (generally described as {110} plane), to which the (210)_{PE} and (310)_{PE} planes is nearly perpendicular, should be in contact with the HOPG (0001) substrate surface. Even

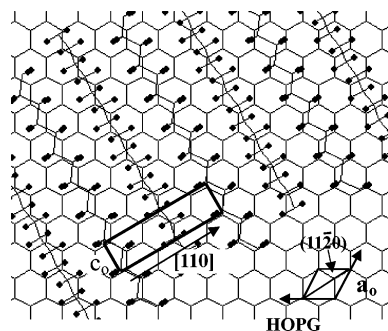


Figure 6. Epitaxial model of PE crystal on HOPG surface: Honeycomb stands for the HOPG lattice, and a set of chain models represents the PE lattice projected onto the $(110)_{\text{PE}}$ plane. Small solid discs denote hydrogen atoms of PE chains. C_0 denotes the repeating period of PE, and the arrow denotes the $[110]_{\text{PE}}$ direction. At the lower-right, the unit cell of a HOPG is depicted.

so, when the fibrillar crystals fluctuate from side to side around their length axis, the 110 reflection could fulfill the reflection condition. It is to be stressed here that the 002_{PE} reflection is observed in the direction parallel to the $11\bar{2}0_{\text{HOPG}}$ reflection. From the above discussion, we reach the same conclusion that was drawn by Tuinstra and Baer⁹ and by Takenaka et al.;¹⁷ molecular chains of PE lay down on the HOPG surface and align in the direction parallel to the $[11\bar{2}0]_{\text{HOPG}}$ direction. In other words, fibrillar PE crystals were overgrown on HOPG with the epitaxial mode; $(110)_{\text{PE}}//(\bar{0}001)_{\text{HOPG}}$ and $\langle 001 \rangle_{\text{PE}}//\langle 11\bar{2}0 \rangle_{\text{HOPG}}$. This epitaxial model is shown in real space in Figure 6. It was also observed that normal paraffin platelets overgrew on the HOPG from the solution, achieving this relationship in orientation.¹⁰ There were also many epitaxial systems on the HOPG, in which PE epitaxially crystallizes on organic and inorganic substrates, with PE chains lying parallel to the substrates.^{20,21}

The epitaxial model of Figure 6 schematizes only the crystallographic relationship in orientation between PE and HOPG lattices. The relative disposition of the PE lattice with respect to the lattice of the HOPG surface is arbitrary. However, it is evident that the c -axis periodicity of the trans-zigzag backbone of the PE chain corresponds with that of the carbon skeleton of HOPG honeycomb. Surely, the corresponding periodicity between two lattices should be the driving force of the epitaxy. On the other hand, the lattice mismatch along the direction normal to the PE chain axis, i.e., the $\langle 110 \rangle_{\text{PE}}$ direction, is rather large as seen from Figure 6. It is not always appropriate to say, however, that the lattice matching would not be achieved in the $\langle 110 \rangle_{\text{PE}}$ direction. Annealing was done at a high temperature, e.g., 126 °C, where the PE lattice was expanded in the $\langle 110 \rangle_{\text{PE}}$ direction more than the HOPG lattice in the corresponding direction.^{22,23} Thus, it is likely that there are fewer mismatches; hence the epitaxial fitting should be feasible in the $\langle 110 \rangle_{\text{PE}}$ direction at the annealing temperature. An interesting issue of the epitaxy is how the $(110)_{\text{PE}}$ plane, on which the trans-zigzag backbone of PE chains are arranged alternating nearly flat-on and edge-on, would be disposed on the HOPG honeycomb lattice. To further understand it, we must take into account the following: The energetic calculation predicts that a single PE chain would deposit preferentially with the trans-zigzag backbone parallel (namely, flat-on) to the substrate,²⁴ and PE crystallizes with the monoclinic form at the PE/HOPG interface.¹⁷ This issue is beyond the object of this paper.

The fine fibrils extending from the edge of the original single crystal in Figure 1 were about 10 nm wide. The width of fibrils ranged from 10 to 20 nm in TEM images in Figures 4 and 5. It

is concluded that the molecular chains should fold back and forth perpendicularly to their length axis. In other words, fibrillar crystals are “chain-folded lamellae” growing edge-on on the substrate. Alkane platelets also grew edge-on on the graphite from the solution, keeping their chain axis parallel to the $[11\bar{2}0]_{\text{HOPG}}$.¹⁰ Though dispersed, the width simply corresponded to the thickness of edge-on lamellae, i.e., the fold period. On annealing on other substrates at a temperature around 126 °C, PE single crystals usually thickened to this range, keeping their original chain orientation to the substrate.^{1,25,26} On annealing on the HOPG substrate, chains laid down onto it, transforming drastically their orientation from a normal orientation to parallel one. The transformation of the chain orientation is specific in annealing on the HOPG substrate. It is not caused by the same mechanism as polymer lamellae made thicker on other substrates by annealing. It is considered that recrystallization from the “partially melted state” must be involved in the growth process of the fine edge-on lamellae. It is known that PE chains are so mobile as to go around quickly on the substrate, e.g., on a glass plate⁶ and a polyethylene crystal,²⁷ at a temperature below melting point in the process of heating. Thus, it is possible that the highly mobile molecular chains crystallize, forming edge-on lamellae, in a similar way as they do from a supercooled melt. In some cases, PE chains could flow out of the interior of lamella and similarly crystallize there to form fine fibrils as seen in Figure 1. On crystallization of polymers from the isotropic melt, the thickness of lamellae depends on the degree of supercooling from the melting point. In reality, when PE is crystallized at 126 °C from the melt, the thickness of lamellae ranges from 20 to 30 nm. The present value (10–20 nm) slightly smaller than that of lamellae grown from the isotropic melt. It is due to the growth of lamellae by the crystallization through the heterogeneous nucleation process, i.e., by epitaxy, on the HOPG substrate. Here, we must pay attention to the observations on melt-crystallized ultralong alkane on HOPG by Tracz and Ungar;¹⁶ the ultralong chain alkane crystallized in an extended conformation and formed the layered structure of bands near the HOPG surface, and folded chains were embedded in chain-extended bands forming far away from the surface. In consideration of this, it is likely even in the present case that thin chain-folded lamellae would not grow directly edge-on on the HOPG surface and that the chain-extended bands would form first on the surface and chain-folded lamellae would grow on it. The morphology of annealed PE single crystals near the HOPG surface is open for further study.

In Figure 7, the original diamond-shaped PE single crystal before annealing can be clearly traced. Fibrils arranged roughly perpendicular to the edges of original diamond shape. The fibrils in neighboring sectors are contiguous at ca. 120° along the a -axis sector boundary, as described above on the morphology of Figure 1. Clearly, the two differently oriented fibrils should attribute to the appearance of the two sets of 110_{PE} reflections. In referring to the electron diffraction pattern in Figure 4, the inset electron diffraction pattern explains again that molecular chains lay down on the substrate and were arranged normally to the length axis of fibrils. In consideration of the orientation of fibrils in annealed single crystal and the molecular orientation within them, a model for venation texture of annealed PE single crystal is schematized as in the parts b and c of Figure 8.

In Figure 8a, the molecular conformation and arrangement in as-grown lamellar crystal are modeled. Reneker and Geil suggested packing models of folds in the $\{110\}$ sector that are now referred to as RGI and RGII packing habit.²⁸ In either situation, molecular chains fold back and forth along the $\{110\}$

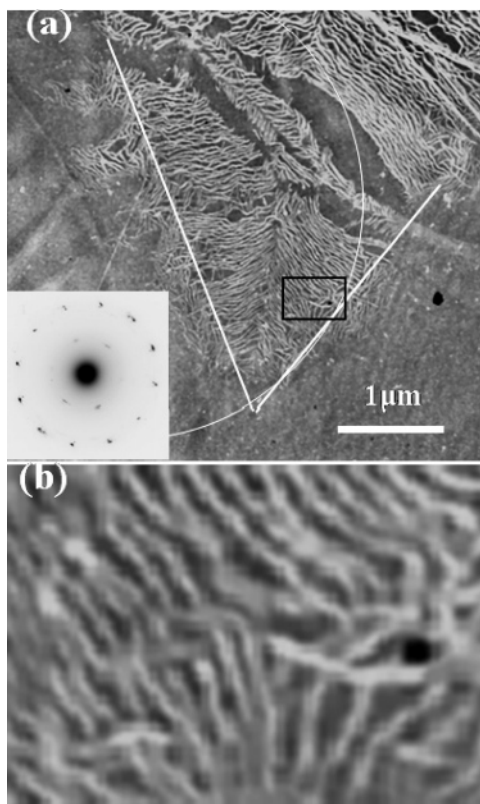


Figure 7. (a) TEM photograph of a PE single crystal annealed on a HOPG at 126 °C. White lines indicate the edges of the original diamond-shaped PE single crystal. Inset is an electron diffraction pattern corresponding to the encircled area. (b) Magnified image of the area enclosed with a rectangle in a.

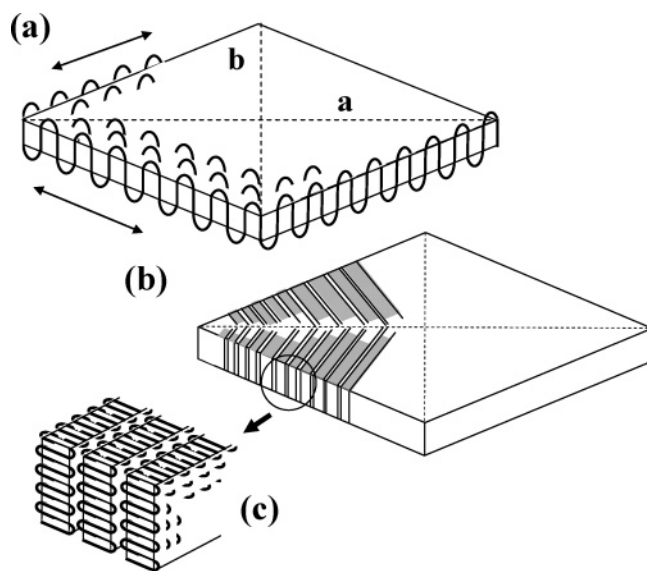


Figure 8. (a) Model of an as-grown PE single crystal. Arrows show the folding direction of chain molecules. Dotted lines marked with characters a and b denote the sector-boundaries along both the crystallographic *a* and *b* axes. (b) Model of an annealed PE single crystal exhibiting a venation texture of edge-on fibrils. Shaded strips represent the edge-on fibrils. (c) Enlargement of the area encircled in part b.

plane. On annealing, chains should lie down toward the direction, along which the chain folds back and forth, and extends along it. This implies that the folds of chain segments in contact with the HOPG substrate should control or affect the lying-down direction of chains on the substrate.

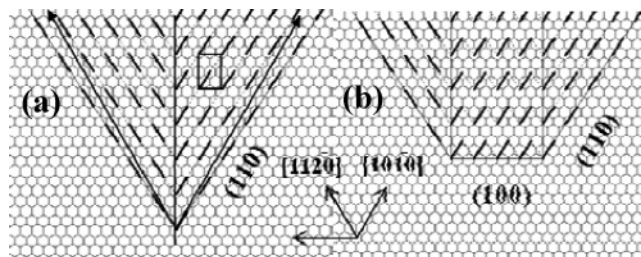


Figure 9. Symmetric disposition of PE single crystal on the HOPG surface: (a) a diamond-shaped single crystal and (b) truncated one. Short thick rods and thin dotted lines represent folds on the top fold surface of a single crystal and ones on the fold surface in contact with the HOPG surface, respectively. The vertical line in part a, which passes through the apex of the diamond-shaped single crystal, shows the *a*-axis sector-boundary. Arrows drawn at an angle of $\pm 60^\circ$ from the apex on both sides with respect to the sector-boundary, designate the direction $\langle 10\bar{1}0 \rangle$ of hexagonal HOPG lattice. Background hexagonal net shows the honeycomb of the HOPG (0001) surface. Vertical thin lines in part b designate the sector-boundaries between $\{110\}$ and $\{200\}$ sectors. In both models, the PE lattice is drawn on the basis of the cell size at room temperature.¹⁹

In Figure 9a, a diamond-shaped single crystal is put on the HOPG substrate in such a symmetric manner as the *a*-axis sector boundary coincides with the $\langle 21\bar{3}0 \rangle$ direction of HOPG substrate, i.e., the vertical direction in the figure. The apex angle of the PE diamond-shaped crystal in the *a*-axis sector-boundary is 67° (the value is calculated using the lattice constants at room temperature¹⁹). In such a disposition, therefore, the folding direction of molecular chains on the right side of original diamond-shape with respect to the sector-boundary is almost parallel to $[10\bar{1}0]_{\text{HOPG}}$ and that on the left side is parallel to the $[11\bar{2}0]_{\text{HOPG}}$. In other words, chain segments of folds fulfill the requisition to the epitaxial fitting in respective sectors as they are (see Figure 6): The chain segments of folds lie down parallel to the HOPG substrate and are directed in the $[10\bar{1}0]_{\text{HOPG}}$ or $[11\bar{2}0]_{\text{HOPG}}$ direction. In Figure 9, the direction of chain folding is widened actually by about 4° from the $[10\bar{1}0]_{\text{HOPG}}$ or $[11\bar{2}0]_{\text{HOPG}}$. This is due to that the PE lattice is drawn using the unit cell at room temperature. Since the PE lattice is thermally expanded more in the *a*-axis direction than in the *b*-axis direction,^{22,23} the apex angle is smaller at higher temperatures where annealing was done. So, it is considered that parallelism of a row of folds is better and epitaxial fitting would be more feasible at the annealing temperature. The symmetrical arrangement of fibrils as in Figure 7 was brought about by annealing when the original diamond-shaped lamella was disposed symmetrically. In considering that the orientation of fibrils is determined by the orientation of the folds to the substrate lattice, it is evident that when a single crystal was disposed asymmetrically and annealed, the resulting fibrillar edge-on lamellae were arranged asymmetrically with respect to the *a*-axis sector boundary.

Figure 9b shows the symmetric disposition of truncated single crystals with respect to the *a*-axis sector boundary. Since the relationship in orientation of the folds to the substrate in the $\{110\}$ sector is the same as described above, the annealing behavior is interpreted similarly. On the contrary, molecular chains fold back and forth along the $\{200\}$ plane in the $\{200\}$ sector. In reality, respective chain segments of folds might be oriented in the $\langle 110 \rangle_{\text{PE}}$, rather than the $\langle 020 \rangle_{\text{PE}}$ direction, in the $\{200\}$ sector. In either case, polymer chains run parallel to the $\langle 020 \rangle_{\text{PE}}$, i.e., parallel to the $[01\bar{1}0]_{\text{HOPG}}$, which is favorable to the present epitaxy, as a whole.²⁹ In the molecular orientation of PE, the epitaxial fitting is ready to be performed, hence, their length axis is oriented parallel to the *a*-axis sector-boundary

when edge-on lamellae are formed with chain folding. In this way, the morphology and orientation of fibrils in the {200} sector as seen in Figure 2 and also in Figure 3 of ref 7 are understood again in terms of the relationship in orientation of the segments of folds to the crystallographic axis of HOPG lattice.

In many cases, fibrils did not always extend parallel to the identical direction over a whole sector. In a typical case, fibrils extend across the sector boundary and their length axis is tilted at the lateral surface of original diamond-shaped lamellar, for example at the right side of annealed lamella in Figure 5. On close examination, we see that fibrils also bend sharply like a crankshaft and change their direction even in one sector, as indicated in the encircled areas of Figure 1 and Figure 5b. Such changes in orientation of fibrils are seen in figures in refs 2 and 4. Fibrils bend at an angle of \pm ca. 60° . In most cases, single crystals are disposed asymmetrically about the *a*-axis sector-boundary. In such an asymmetrical disposition of a single crystal on the HOPG, fold segments could not be in contact with the HOPG in such a way as they could take the parallel orientation to the $[10\bar{1}0]_{\text{HOPG}}$ or $[01\bar{1}0]_{\text{HOPG}}$ direction. On annealing the obstructed single crystal's orientation, the chains would also lie down and extend, but they would both take the orientation preferable to performing the epitaxy. Then, the preferred orientations are the directions of the HOPG lattice, along which the epitaxy is feasible and differ by $\pm 60^\circ$, e.g. $[10\bar{1}0]_{\text{HOPG}}$ and $[10\bar{2}0]_{\text{HOPG}}$. As a result, the, fibrils bend by changing the direction of epitaxial performance in the process of growing.

Concluding Remarks

When polymer single crystals are annealed on a substrate, with which polymer crystals have no special crystallographic affinity, they thicken and are reorganized keeping their original molecular orientation. In the present experiment, it was found that when PE single crystals were annealed on the HOPG, molecular chains laid down on the substrate, performing the epitaxial orientation. In the epitaxial orientation, the folding direction of chains in an original lamella controlled the direction in which PE chains laid down and extended in the annealed crystal. It was also found that when PE single crystals were annealed on an oriented polypropylene film, molecular chains were rearranged to perform epitaxial matching with the polypropylene substrate, keeping their normal orientation to the substrate surface.⁴ When polymers are crystallized on many organic and inorganic substrates *from the melt or solution*, the oriented overgrowth of crystals takes place to perform the lattice matching between the crystal and the substrate. However, on the substrate with which polymer crystals have strong affinity crystallographically, single crystals of polymers are reorganized

epitaxially by annealing at a temperature below the melting point. The molecular orientation is crystallographically adjusted to the substrate *through partial melting*, performing lattice matching between the polymer crystal and the substrate.

References and Notes

- (1) Geil, P. H. *Polymer Single Crystals*; Wiley-Interscience: New York, 1963. Wunderlich, B. *Macromolecular Physics Volume 1 (Crystal structure, morphology, defects)*; Academic Press: New York, 1973. Bassette, D. C. *Principles of Polymer Morphology*; Cambridge University Press, U.K., 1981. Somer, J.-U., Reiter, G., Eds. *Polymer Crystallization*; Springer-Verlag: Heidelberg, Germany, 2003.
- (2) Maganov, S. N.; Yerina, N. A.; Ungar, G.; Reneker, D. H.; Ivanov, D. A. *Macromolecules* **2003**, *36*, 5637–5649.
- (3) Dubreuil, N.; Hocquet, S.; Dosièrre, M.; Ivanov, D. A. *Macromolecules* **2004**, *37*, 1–5.
- (4) Nakamura, J.; Kawaguchi, A. *Macromolecules* **2004**, *37*, 3725–3734.
- (5) Organ, S. J.; Hobbs, J. K.; Miles, M. J. *Macromolecules* **2004**, *37*, 4562–4572.
- (6) Sanz, N.; Hobbs, J. K.; Miles, M. J. *Langmuir* **2004**, *20*, 5989–5997.
- (7) Magonov, S. N.; Yerina, N. A.; Godovsky, Y.; Reneker, D. H. *J. Macromol. Sci., Part B: Phys.* **2006**, *45*, 169–194.
- (8) Gearba, R. I.; Dubreuil, N.; Anokhin, D. V.; Godovsky, Y. K.; Ruan, Jr.-J.; Thierry, A.; Lotz, B.; Ivanov, A. D. *Macromolecules* **2006**, *39*, 978–987.
- (9) Tuinstra, F.; Baer, E. *J. Polym. Sci., Polym. Lett. Ed.* **1970**, *8*, 861–865.
- (10) Boucher, E. A. *J. Mater. Sci.* **1973**, *8*, 146–148.
- (11) Rabe, J. P.; Buchholz, S. *Science* **1991**, *253*, 424–427.
- (12) Magonov, S. N.; Whango, M.-H. *Surface Analysis with STM and AFM*; VCH Publishers: Weinheim, Germany, 1996.
- (13) Percec, V.; Rudick, J. G.; Wagner, M.; Obata, M.; Mitchell, C. M.; Cho, W.-D.; Maganov, S. N. *Macromolecules* **2006**, *39*, 7342–7351.
- (14) Tracz, A.; Jeszka, J. K.; Kucinska, I.; Chapel, J.-P.; Boiteux, G.; Kryszewski, M. *J. Appl. Polym. Sci.* **2002**, *86*, 1329–1336.
- (15) Tracz, A.; Kucinska, I.; Jeszka, J. K. *Macromolecules* **2003**, *36*, 10130–10132.
- (16) Tracz, N.; Ungar, G. *Macromolecules* **2005**, *38*, 4962–4965.
- (17) Takenaka, Y.; Miyaji, H.; Hoshino, A.; Tracz, A.; Jeszka, J. K.; Kucinska, I. *Macromolecules* **2004**, *37*, 9667–9669.
- (18) Blundell, D. J.; Keller, A.; Kovacs, A. I. *Polym. Lett.* **1966**, *4*, 481–486.
- (19) Bunn, C. W. *Trans. Faraday Soc.* **1939**, *35*, 482–490.
- (20) Mauritz, K. A.; Baer, E.; Hopfinger, A. J. *J. Polym. Sci. Macromol. Rev.* **1978**, *13*, 1–61.
- (21) Lotz, B.; Wittmann, J. C. *J. Polym. Sci., Polym. Phys.* **1986**, *24*, 1541–1558.
- (22) Swan, P. W. *J. Polym. Sci.* **1962**, *56*, 403–407.
- (23) Davis, G. T.; Eby, R. K.; Colson, J. P. *J. Appl. Phys.* **1970**, *41*, 4316–4326.
- (24) Baukema, P. R.; Hopfinger, A. J. *J. Polym. Sci., Polym. Phys. Ed.* **1982**, *20*, 399–409.
- (25) Statton, W. O.; Geil, P. H. *J. Appl. Polym. Sci.* **1960**, *3*, 357–361.
- (26) Kawaguchi, A.; Ichida, T.; Murakami, S.; Katayama, K. *Colloid Polym. Sci.* **1984**, *262*, 597–604.
- (27) Taniguchi, N.; Kawaguchi, A. *Macromolecules* **2005**, *38*, 4761–4768.
- (28) Reneker, D. H.; Geil, P. H. *J. Appl. Phys.* **1960**, *31*, 1916–1925.
- (29) Discussed in detail by Davé, R. S.; Farmer, B. L. *Polymer* **1988**, *29*, 1544–1554.

MA071674Y